

Article

# Circulant Singular Spectrum Analysis to Monitor the State of the Economy in Real Time

Juan Bógalo <sup>1</sup>, Pilar Poncela <sup>1</sup> and Eva Senra <sup>2,\*</sup>

<sup>1</sup> Departamento de Análisis Económico, Economía Cuantitativa, Facultad de Económicas, Universidad Autónoma de Madrid, 28049 Madrid, Spain; juan.bogalo@uam.es (J.B.); pilar.poncela@uam.es (P.P.)

<sup>2</sup> Departamento de Economía, Facultad C.C. Economía, Empresariales y Turismo, Universidad de Alcalá, 28802 Alcalá de Henares, Spain

\* Correspondence: eva.senra@uah.es

**Abstract:** Real-time monitoring of the economy is based on activity indicators that show regular patterns such as trends, seasonality and business cycles. However, parametric and non-parametric methods for signal extraction produce revisions at the end of the sample, and the arrival of new data makes it difficult to assess the state of the economy. In this paper, we compare two signal extraction procedures: Circulant Singular Spectral Analysis, CiSSA, a non-parametric technique in which we can extract components associated with desired frequencies, and a parametric method based on ARIMA modelling. Through a set of simulations, we show that the magnitude of the revisions produced by CiSSA converges to zero quicker, and it is smaller than that of the alternative procedure.

**Keywords:** ARIMA; business cycle; CiSSA; revision



**Citation:** Bógalo, J.; Poncela, P.; Senra, E. Circulant Singular Spectrum Analysis to Monitor the State of the Economy in Real Time. *Mathematics* **2021**, *9*, 1169. <https://doi.org/10.3390/math9111169>

Academic Editors: María-Isabel Ayuda and María Dolores Gadea Rivas

Received: 15 April 2021  
Accepted: 19 May 2021  
Published: 22 May 2021

**Publisher's Note:** MDPI stays neutral with regard to jurisdictional claims in published maps and institutional affiliations.



**Copyright:** © 2021 by the authors. Licensee MDPI, Basel, Switzerland. This article is an open access article distributed under the terms and conditions of the Creative Commons Attribution (CC BY) license (<https://creativecommons.org/licenses/by/4.0/>).

## 1. Introduction

Real-time monitoring of the economy is key to assess the state of the business cycle [1]. Unfortunately, business cycle signals are subject to revisions, and this might condition the real-time decisions taken by economic policy authorities [2]. This has motivated the central banks' interest in revisions, for instance, as shown by the Bank of England [3], the European Central Bank [4] or the Federal Reserve [5].

The literature on data revision is related to the analysis of real-time data [1,6,7]. As [8] points out, institutions are reluctant to enact large data revisions, and therefore analysts value signal extraction methods that necessitate few revisions. There are two causes for revising the estimates of the extracted signals: to adjust to the new information incorporated in "old", already published data (of periods  $s < t$ ), or to update the estimates of the unobserved signal due to the appearance of new data in the following periods,  $s > t$ . The first cause of data revisions has been widely analyzed in the literature, for instance, in [7,9,10] or earlier references such as [11–14]. The second cause for updating the extracted signals has been analyzed in [15], and Refs. [8,16] make partial comparisons of different alternatives. We add to this literature by analyzing how posterior published data affect the estimated signals by comparing two procedures: a parametric ARIMA-model-based approach widely used by statistical offices (Tramo-Seats, see for instance [17]) and a non-parametric procedure based on Singular Spectrum Analysis, SSA, recently introduced in [18]. Though revisions are inherent to any moment in time, they are crucial when there is a business cycle turning point or abrupt changes in the data generation process [19,20], like the ones currently witnessed due to COVID-19. It is at these times when non-parametric signal extraction procedures become very valuable and provide a more robust signal.

Circulant Singular Spectrum Analysis, CiSSA, is a non-parametric procedure that allows one to automatically decompose any economic time series into trend, seasonal and business cycle components [18]. CiSSA relies on traditional Singular Spectrum Analysis,

SSA, a non-parametric procedure based on subspace algorithms [21]. Its applications cover many time series problems like signal extraction, forecasting, and missing value imputation, among others [22–24]. SSA performs the singular value decomposition of the so-called trajectory matrix, which is built by putting together lagged pieces of the original time series. Basic SSA was introduced by [25,26]. A theoretical variation based on Toeplitz matrices for stationary time series was developed in [27]. A diagonal averaging procedure needed to reconstruct the time series in the final step is proposed by [28]. Very recently, [18] introduces CiSSA, linking the eigen decomposition to the frequency of the extracted signals and proving the asymptotic equivalence of the three variants (Basic, Toeplitz and Circulant SSA). SSA is widely applied across fields like biometrics, climatology, energy and volcanic activity, among others [29–32]. Applications in economics cover the analysis of business cycles, volatility estimation and forecasting [10,33,34].

Signals estimated with alternative versions of SSA are also affected by revisions at the end of the sample when including new information. However, the literature on data revisions with SSA is scarce. In fact, since the origin of SSA [25,26], 25 years elapsed before the appearance of the first study on SSA revisions [9]. Initial studies focused on published data revisions, considering the successive waves of data publications (vintages) as different time series in a multivariate framework, a methodology that had been introduced by [35]. In [10,36] the focus is on revisions caused by the recalculation of the extracted signal when additional data appear in the following periods. The revisions for US GDP obtained by SSA are compared with those calculated by some univariate filters in [10] and in a multivariate setup for US IP in [36]. Both papers compare the initial estimate with the final one, based on the quasi-real estimate given in [15].

In this paper, we study the evolution of the revisions, period by period, until reaching the final estimate, with the objective of analyzing the impact of any economic event on the posterior estimation of the business cycle. Since there are no observed data on the business cycle, in a first step we perform a set of simulations of linear and non-linear models and compare the revisions of CiSSA with those of a parametric approach, such as ARIMA-model-based, AMB, methods. In the second step, we check how revisions affect future forecasts of measured or observed time series when using unobserved component models. We introduce an alternative concept of final estimation, following [37] to avoid distortions, because, according to the one used by [15], the time elapsed from the first estimate of the underlying component to the so-called final one is not the same for all available data in a particular time. We conclude that the business cycle estimates made with ARIMA models suffer greater revisions than those made with Circulant SSA.

This paper contributes to the existing literature on the effect of data revisions in signal extraction in several aspects: first, we show that CiSSA signal estimations at the end of the sample are asymptotically unbiased as new data arrive; second, we characterize the magnitude of data revisions with CiSSA; third, we provide a comparison of the relative performance with an AMB parametric signal extraction procedure. We do so through simulations in a linear and non-linear setup and, finally, through a data set in a real-time application.

The rest of the paper is organized as follows. In Section 2, we describe the different approaches to estimate the business cycle and compare revisions. In Section 3, we carry out our simulation study to compare the revisions made with non-parametric SSA versus parametric, based on ARIMA models. We complement the analysis with an application to real data. Finally, in Section 4, we conclude.

## 2. Methodology

In this section we describe the two alternative procedures, non-parametric and parametric, that we use to estimate the business cycle: Circulant SSA and an ARIMA-model-based decomposition. As is seen in the literature [10], the trend-cycle component is formed by all the oscillatory fluctuations of a period greater than one year and a half. There are two alternatives to estimate the business cycle: to directly estimate it or, alternatively, to consider the first differences of a joint trend-cycle component. Given that AMB procedures

are not able to differentiate the trend from the cycle [38], we follow the second path. Thus, the business cycle estimate  $\hat{c}_t$  is given by

$$\hat{c}_t = y_t - y_{t-1}$$

where  $y_t$  is the trend-cycle component. In what follows, we describe both approaches.

### 2.1. Circulant Singular Spectrum Analysis

CiSSA is an algorithm that decomposes the original time series into the sum of a set of oscillatory components at known frequencies. Its main advantage is that users can group the extracted components according to their needs because those components are precisely identified by frequency. CiSSA can be applied to stationary and non-stationary time series, as Theorem 2 in [18] states. However, for simplicity in presenting the method, let us assume that  $\{x_t\}$  is a zero mean stationary time series of length  $T$ , given in the vector  $\mathbf{x} = (x_1, \dots, x_T)'$ , and let  $L$  be a positive integer, called window length, such that  $L < T/2$ . The four steps of any SSA signal extraction procedure adapted to Circulant SSA, as described in [18], are as follows:

- Step 1: Build the trajectory matrix.

From the original time series, we obtain the  $L \times N$  trajectory matrix  $\mathbf{X}$ , given by  $L$  time series of length  $N = T - L + 1$  as

$$\mathbf{X} = (\mathbf{x}_1 | \dots | \mathbf{x}_N) = \begin{pmatrix} x_1 & x_2 & \dots & x_N \\ x_2 & x_3 & \dots & x_{N+1} \\ \vdots & \vdots & \ddots & \vdots \\ x_L & x_{L+1} & \dots & x_T \end{pmatrix}$$

where  $\mathbf{x}_j = (x_j, \dots, x_{j+L-1})'$  is the vector of dimension  $L$  and origin at time  $j$ . The matrix  $\mathbf{X}$  is Hankel, and both by columns and by rows we have subseries of the original time series  $\{x_t\}$ .

- Step 2: Decomposition.

We project the trajectory matrix over the space spanned by a set of eigenvectors to obtain the unobserved components. To do so, first we build the circulant matrix,  $\mathbf{S}_C$ , from the sample second moments:

$$s_m = \frac{1}{T - m} \sum_{t=1}^{T-m} x_t x_{t-m}, \quad m = 0, 1, \dots, L - 1.$$

The elements of the first row in  $\mathbf{S}_C$ ,  $\boldsymbol{\alpha} = (\alpha_0, \alpha_1, \dots, \alpha_{L-1})$ , are defined as

$$\alpha_m = \frac{L - m}{L} s_m + \frac{m}{L} s_{L-m}, \quad m = 0, 1, \dots, L - 1$$

The eigenvalues of  $\mathbf{S}_C$  are given by  $\text{diag}(\lambda_1, \dots, \lambda_L) = \mathbf{U}^* \mathbf{S}_C \mathbf{U}$ , where  $\mathbf{U}$  is the Fourier unit matrix and  $\mathbf{A}^*$  denotes the conjugate transpose of  $\mathbf{A}$ . The  $k$ -column of  $\mathbf{U}$  is the eigenvector associated to the eigenvalue  $\lambda_k$ , given by  $\mathbf{u}_k = L^{-1/2} (u_{k,1}, \dots, u_{k,L})'$  with  $u_{k,j} = \exp(-i2\pi(j - 1) \frac{k-1}{L})$ . Additional details are specified in [18]. The eigenvalues  $\lambda_k$  are estimations of the spectral density of the time series  $x_t$  for the frequency  $\omega_k = \frac{k-1}{L}$ ,  $k = 1, \dots, L$ , since

$$\lambda_k \simeq \hat{f}\left(\frac{k-1}{L}\right) = \sum_{m=-\infty}^{\infty} s_m \exp\left(i2\pi m \frac{k-1}{L}\right)$$

Therefore, there is a direct relationship between the eigenvalue  $\lambda_k$  and the frequency  $\omega_k = \frac{k-1}{L}$ .

In this way we can decompose the trajectory matrix  $\mathbf{X}$  as sum of the elementary matrices  $\mathbf{X}_k$  of rank 1, that is,

$$\mathbf{X} = \sum_{k=1}^L \mathbf{X}_k = \sum_{k=1}^L \mathbf{u}_k \mathbf{u}_k^* \mathbf{X}$$

- Step 3: Grouping.

The spectral density function is symmetric, therefore,  $\lambda_k = \lambda_{L+2-k}$ , and the corresponding eigenvectors are complex conjugates,  $\mathbf{u}_k = \bar{\mathbf{u}}_{L+2-k}$ ; that is, the elementary matrices  $\mathbf{X}_k$  and  $\mathbf{X}_{L+2-k}$  are associated with the same frequency, and we group them together in the elementary pairs of frequencies  $B_k = \{k, L + 2 - k\}$  for  $k = 2, \dots, G$ , with  $B_1 = \{1\}$  and  $B_{\frac{L}{2}+1} = \{\frac{L}{2} + 1\}$  if  $L$  is even, where  $G = \lfloor \frac{L+1}{2} \rfloor$ , with  $\lfloor \cdot \rfloor$  being the integer part.

We compute the elementary matrices by frequencies,

$$\begin{aligned} \mathbf{X}_{B_k} &= \mathbf{X}_k + \mathbf{X}_{L+2-k} \\ &= \mathbf{u}_k \mathbf{u}_k^* \mathbf{X} + \mathbf{u}_{L+2-k} \mathbf{u}_{L+2-k}^* \mathbf{X} \\ &= (\mathbf{u}_k \mathbf{u}_k^* + \bar{\mathbf{u}}_k \bar{\mathbf{u}}_k^*) \mathbf{X} \\ &= 2(\mathcal{R}_{\mathbf{u}_k} \mathcal{R}'_{\mathbf{u}_k} + \mathcal{I}_{\mathbf{u}_k} \mathcal{I}'_{\mathbf{u}_k}) \mathbf{X} \end{aligned}$$

where  $\mathcal{R}_{\mathbf{u}_k} = \text{real}(\mathbf{u}_k)$  and  $\mathcal{I}_{\mathbf{u}_k} = \text{imag}(\mathbf{u}_k)$ , so both  $\mathbf{X}_k$  and  $\mathbf{X}_{B_k}$  are real.

We link the different elementary groups by frequencies  $B_k$  to an unobserved component (trend, cycle, . . . ) according to the goal of our analysis. The matrix associated with a desired unobserved component  $I_j$  is the sum of the matrices associated with all frequencies that defined that component  $\mathbf{X}_{I_j} = \mathbf{X}_{B_{k1}} + \dots + \mathbf{X}_{B_{kp}}$ . Finally, the trajectory matrix can be recovered as  $\mathbf{X} = \mathbf{X}_{B_1} + \dots + \mathbf{X}_{B_G}$ . The contribution of a particular elementary group by frequency  $B_k$  is given by  $2\lambda_k / \sum \lambda_k$  for  $k = 2, \dots, G$  and  $\lambda_1 / \sum \lambda_k$  for  $k = 1$ .

- Step 4: Reconstruction.

In this step, we have to transform the matrices  $\mathbf{X}_{I_j} = (x_{ik}^{(j)})$ , computed in the previous steps, in time series of length  $T$ ,  $\tilde{\mathbf{x}}^{(j)} = (\tilde{x}_1^{(j)}, \dots, \tilde{x}_T^{(j)})'$ . We call this series reconstructed series, and it is given by diagonal averaging as

$$\tilde{x}_t^{(j)} = \begin{cases} \frac{1}{t} \sum_{i=1}^t x_{i,t-i+1}^{(j)} & 1 \leq t < L \\ \frac{1}{L} \sum_{i=1}^L x_{i,t-i+1}^{(j)} & L \leq t \leq N \\ \frac{1}{T-t+1} \sum_{i=t-T+L}^L x_{i,t-i+1}^{(j)} & N < t \leq T \end{cases}$$

A block diagram presenting the several stages of the calculations in CiSSA is presented in Figure 1. As it can be seen, the only parameter to apply CiSSA is the window length  $L$ . To select this value, there is one general rule,  $L < T/2$ , because otherwise the trajectory matrices with window length  $L$  and  $N = T - L + 1$  are equivalent. Other rules can be found in the literature: on the one hand,  $L \leq T/3$  to have enough observations to estimate the sample second moments [28]; in addition, it has to be large enough to describe a trend with a complex structure and to preclude producing components with mixed-frequencies, and it should be a multiple of the seasonal periodicity and of the period of any oscillatory component that is necessary for extraction [21].

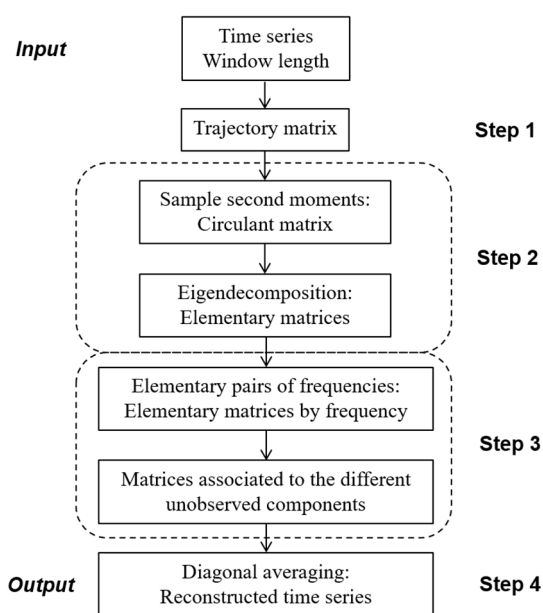


Figure 1. Block diagram presenting the several stages of CiSSA.

2.2. ARIMA-Model-Based Procedure

Assume now that the non-stationary time series  $x_t$  has  $d$  and  $D$  regular and seasonal unit roots, respectively. Let  $s$  be the seasonal period and  $B$  the backwards operator such that  $B^h x_t = x_{t-h}$ . Then, as it is well known, the seasonal multiplicative ARIMA model is given by

$$\phi_p(B)\Phi_P(B)\nabla^d\nabla_s^D x_t = \theta_q(B)\Theta_Q(B)a_t$$

or equivalently,

$$x_t = \frac{\theta_q(B)\Theta_Q(B)}{\phi_p(B)\Phi_P(B)\nabla^d\nabla_s^D} a_t = \psi(B)a_t \tag{1}$$

where  $\phi_p(B) = 1 - \phi_1 B - \dots - \phi_p B^p$  is the autoregressive polynomial of the regular part of order  $p$ ,  $\Phi_P(B^s) = 1 - \Phi_1 B^s - \dots - \Phi_P B^{sP}$  is the autoregressive polynomial of the seasonal part of order  $P$ ,  $\nabla^d = (1 - B)^d$  and  $\nabla_s^D = (1 - B^s)^D$  are the regular and seasonal differences, respectively,  $\theta_q(B) = 1 - \theta_1 B - \dots - \theta_q B^q$  is the moving average polynomial of the regular part of order  $q$ ,  $\Theta_Q(B^s) = 1 - \Theta_1 B^s - \dots - \Theta_Q B^{sQ}$  is the moving average polynomial of the seasonal part of order  $Q$ , and  $a_t$  is white noise with variance  $\sigma_a^2$ .

Given the ARIMA model for the original time series, a signal extraction decomposition of the time series in trend-cycle, seasonal and irregular components is proposed in [39] by deriving the corresponding ARIMA models for the components. Their Minimum Mean Square Error (MMSE) estimators are given by the application of Wiener-Kolmogorov filters to the original time series. In the case of the trend-cycle component ( $Y$ ), the filter is given by

$$WK(B, F) = \frac{\psi_Y(B)\psi_Y(F)}{\psi(B)\psi(F)}$$

where  $F = B^{-1}$  is the forward operator,  $\psi(B)$  is given in (1) and  $\psi_Y(B)$  is the corresponding derived ARIMA model for the trend-cycle component. Wiener-Kolmogorov filters are symmetric and centered. These filters were derived by Kolmogorov [40] and Wiener [41] for stationary time series. Furthermore, it is shown that they are valid for the nonstationary case in [42].

2.3. Revisions

We focus on the end-of-sample revisions due to the signal re-estimations caused by the release of new data. First, we need to understand the nature of the revisions. In

CiSSA, which is non-parametric, the revision is due to the introduction of new data in the reconstruction stage, while in the ARIMA-based-model procedure, the source of revisions relies both on new parameter estimations and on the update of the forecasts needed to apply the Wiener–Kolmogorov filters.

In what follows, we formalize the process of data revisions. Given data up to time  $t$  of the time series,  $\{x_t\}$ , the initial or concurrent estimate of the business cycle,  $c_t$ , for that period is denoted by  $\hat{c}_{t|t}$ . As new data are available at time  $t + 1, t + 2, \dots$ , we can re-compute the estimation of  $c_t$  and denote it as  $\hat{c}_{t|t+1}, \hat{c}_{t|t+2}, \dots$ . We end up with the procedure after  $K$  periods,  $\hat{c}_t = \hat{c}_{t|t+K}$ , when no more revisions are given. The set formed by the so-called initial, subsequent, and final estimates is the estimation path of the desired component at period  $t$ .

The number of periods  $K$  is by nature different to CiSSA and AMB approaches. On the one hand, in CiSSA, given a window of length  $L$ , the eigenvectors are fixed, so that the projections of the original series for the final period do not change when new data is published in later periods. However, for the final period, the data reconstructed by the diagonal average varies until at least  $L - 1$  new subsequent data are published. Therefore, CiSSA revisions will stop at most after  $K = L - 1$  periods. On the other hand, AMB revisions could last forever, due to parameter re-estimation, though, in practice, it is observed that they usually end between two and five years [37]. To fix a common horizon for both methodologies, and given that  $L$  in CiSSA must be such that  $L < T/2$ , we consider the same value  $K = L$  in both cases.

The difference between a preliminary estimate of the cycle and its final estimate measures the revision that the real-time estimate undergoes. The revision is the measurement error of a preliminary estimate, that is,

$$r_{t|t+j} = \hat{c}_{t|t+j} - \hat{c}_t$$

Considering these for  $j = 0, 1, \dots, K - 1$ , we have the evolution of the revisions from the initial to the final estimation of the cycle.

Notice that the first period for which we have the complete estimation path is  $t_0 = 2L + 1$  and the last one is  $t_1 = T - K = T - L + 1$ . In this way, we have  $P = T - 3L + 1$  preliminary estimates  $j$  periods after the initial estimate,  $j = 0, 1, \dots, K - 1$ .

Figure 2 illustrates the calculation scheme of the preliminary estimates or revisions with  $T = 16$  and  $L = 4$ . For each period, preliminary estimates are available based on the last published period. The dark gray diagonal contains  $P = T - 3L + 1 = 5$  concurrent estimates; in each diagonal of lighter gray color there are the estimates after  $j$  periods; finally, the dashed diagonal shows the final estimates.

The definition of the final estimate used refers to the period from which the estimation of a component does not undergo any more revisions [37], as opposed to the final estimate of [15], which refers to the last available estimate.

Revisions for a time series  $\{x_t\}$  of length  $T$  are obtained by means of a recursive procedure from time  $t_0$  until the end of the sample. First, we take the series up to time  $t_0$  and estimate the cycle, getting the initial estimate for time  $t_0, \hat{c}_{t_0|t_0}$ ; we add a new data point from one more period,  $t_0 + 1$ , and estimate the cycle, getting the initial estimate for time  $t_0 + 1$  and the first preliminary estimation for  $t_0, \hat{c}_{t_0|t_0+1}$ ; we add one more data point,  $t_0 + 2$ , and we estimate the cycle, obtaining the initial estimate for the observation at  $t_0 + 2$ , the first preliminary estimate for  $t_0 + 1$  and the second preliminary estimate for  $t_0, \hat{c}_{t_0|t_0+2}$ ; similarly, we add periods successively until we reach the last available observation. Therefore, for a given  $j$ , we have a sample of size  $P = t_1 - t_0 + 1$  of preliminary estimations  $j$  periods after the initial estimate generated by the set of revisions  $\left\{ r_{t|t+j} \right\}_{t=t_0}^{t_1}$  for  $j = 0, 1, \dots, K - 1$ .

The magnitude of the revisions after  $j$  periods is measured by their standard deviation,  $\sigma(r_{t|t+j})$ . Consequently, the magnitude of the revisions of the business cycle given by the CiSSA and AMB methodologies can be compared by the ratio of their standard deviations,

$$RMR_j = \frac{\sigma(r_{t|t+j}^{CiSSA})}{\sigma(r_{t|t+j}^{AMB})}, j = 0, 1, \dots, K - 1, \tag{2}$$

where  $r_{t|t+j}^{CiSSA}$  and  $r_{t|t+j}^{AMB}$  are the revisions after  $j$  periods generated by the CiSSA and AMB methods, respectively. If for a given  $j$ ,  $RMR_j$  is less than 1, then the revisions with CiSSA will be smaller than those of the AMB method in the preliminary estimation after  $j$  periods of the initial estimation.

		Last available period							
Period		9	10	11	12	13	14	15	16
⋮		⋮	⋮	⋮	⋮	⋮	⋮	⋮	⋮
9		$\hat{c}_{9 9}$	$\hat{c}_{9 10}$	$\hat{c}_{9 11}$	$\hat{c}_{9 12}$	$\hat{c}_9$	$\hat{c}_9$	$\hat{c}_9$	$\hat{c}_9$
10			$\hat{c}_{10 10}$	$\hat{c}_{10 11}$	$\hat{c}_{10 12}$	$\hat{c}_{10 13}$	$\hat{c}_{10}$	$\hat{c}_{10}$	$\hat{c}_{10}$
11				$\hat{c}_{11 11}$	$\hat{c}_{11 12}$	$\hat{c}_{11 13}$	$\hat{c}_{11 14}$	$\hat{c}_{11}$	$\hat{c}_{11}$
12					$\hat{c}_{12 12}$	$\hat{c}_{12 13}$	$\hat{c}_{12 14}$	$\hat{c}_{12 15}$	$\hat{c}_{12}$
13						$\hat{c}_{13 13}$	$\hat{c}_{13 14}$	$\hat{c}_{13 15}$	$\hat{c}_{13}$
14							$\hat{c}_{14 14}$	$\hat{c}_{14 15}$	$\hat{c}_{14 16}$
15								$\hat{c}_{15 15}$	$\hat{c}_{15 16}$
16									$\hat{c}_{16 16}$

Figure 2. Computation scheme of preliminary estimates or revisions for  $T = 16$  and  $L = 4$ .

### 3. Simulations

In this section we check the relative accuracy of the non-parametric, CiSSA, and parametric, AMB, methodologies by means of evaluating the magnitude of the revisions through simulations. However, as revisions are calculated as the differences to a final estimation, we previously check that (1) the final point estimation of the cycle is unbiased,  $E(\hat{c}_{t|t+K}) = c_t$ , and (2) the preliminary point estimations converge to the final estimation.

Simulations are run for linear and non-linear structural models.

#### 3.1. Simulated Models

First, we consider the following linear structural model for a time series  $\{x_t\}$ :

$$x_t = \mu_t + c_t + \gamma_t + \varepsilon_t$$

where  $\mu_t$  is the trend,  $c_t$  the cycle,  $\gamma_t$  are the seasonal components, and  $\varepsilon_t$  is the error term. We assume that the trend follows an integrated random walk as in [43], defined by

$$\begin{aligned} \mu_t &= \mu_{t-1} + \nu_{t-1} \\ \nu_t &= \nu_{t-1} + \xi_{t-1} \quad \xi_t \sim N(0, \sigma_\xi^2) \end{aligned} \tag{3}$$

The models for the cycle and seasonal components follow [44]. The cycle is the first series in a bivariate VAR(1) model, given by

$$\begin{pmatrix} c_t \\ \tilde{c}_t \end{pmatrix} = \rho_c \begin{pmatrix} \cos(2\pi\omega^c) & \sin(2\pi\omega^c) \\ -\sin(2\pi\omega^c) & \cos(2\pi\omega^c) \end{pmatrix} \begin{pmatrix} c_{t-1} \\ \tilde{c}_{t-1} \end{pmatrix} + \begin{pmatrix} \zeta_t \\ \tilde{\zeta}_t \end{pmatrix}, \begin{pmatrix} \zeta_t \\ \tilde{\zeta}_t \end{pmatrix} \sim N(0, \sigma_\zeta^2 \mathbf{I}_2), \tag{4}$$

where the frequency  $\omega^c \in [0, 1]$  and the period is  $1/\omega^c$ . The seasonal component of period  $s$  is given by

$$\gamma_t = \sum_{j=1}^{\lfloor s/2 \rfloor} \left( \eta_{j,t} \cos(2\pi\omega_j^\gamma t) + \tilde{\eta}_{j,t} \sin(2\pi\omega_j^\gamma t) \right), \omega_j^\gamma = \frac{j}{s}, j = 1, \dots, \lfloor s/2 \rfloor, \tag{5}$$

where the coefficients  $\eta_{j,t}$  y  $\tilde{\eta}_{j,t}$  are random walks with noise variances equal to  $\sigma_\zeta^2$  for all the frequencies  $\omega_j^\gamma$ . Finally, the error term  $\varepsilon_t$  is a white noise process  $N(0, \sigma_\varepsilon^2)$ . All the components are independent of one another. We set  $\rho_c = 1$  so the trend and the seasonal and cycle components have a unit root. We consider monthly time series with  $s = 12$ , and the cycle period is equal to  $1/\omega^c = 48$  months.

The non-linear model considered is the one proposed in [44] for UK travelers, given by

$$x_t = \mu_t + c_t + \exp(a_0 + a_1\mu_t)\gamma_t + \varepsilon_t$$

where the trend  $\mu_t$ , the cycle  $c_t$  and the seasonal component  $\gamma_t$  are specified as in Equations (3), (4) and (5), respectively. The constant  $a_0$  scales the seasonal effect, and the constant  $a_1$  determines the sign and the size of the variation when there is a positive change in the trend. The amplitude of the seasonal component is modulated by the combination of  $a_0 + a_1\mu_t$ .

### 3.2. Simulation Results

We perform 1000 simulations for the previous linear and non-linear models with both approaches. All the calculations are run in Matlab (R2021a) (the Matlab functions to run TRAMO-SEATS and CiSSA can be found at [https://es.mathworks.com/matlabcentral/fileexchange/50466-ts-function-tramo-seats-under-matlab?s\\_tid=srchtitle](https://es.mathworks.com/matlabcentral/fileexchange/50466-ts-function-tramo-seats-under-matlab?s_tid=srchtitle) (accessed on 21 May 2021) and [https://es.mathworks.com/matlabcentral/fileexchange/84094-cissa-circulant-ssa-under-matlab?s\\_tid=srchtitle](https://es.mathworks.com/matlabcentral/fileexchange/84094-cissa-circulant-ssa-under-matlab?s_tid=srchtitle) (accessed on 21 May 2021), respectively). For CiSSA, we set two window sizes,  $L = 96$  and  $L = 192$ , proportional to the periodicity of the simulated cycle. To implement the AMB procedure, we chose the automated, widely used Tramo-Seats, TS, [45]. The length for the simulated series is  $T = 3L + P - 1$ , where  $P$  is the number of available observations of  $r_{t|t+j}$  for a given  $j$ . To be consistent with the maximum length allowed by Tramo-Seats,  $T = 600$ , we take  $P = 100$  for  $L = 96$  and  $P = 25$  with  $L = 192$  (notice that these two values for  $L$  are multiples of the simulated seasonality and cycle and are smaller than  $T/3$ , following the criteria for selecting  $L$  given at the end of Section 2.1). The maximum duration of the revision process is  $K = L - 1$ , for both methods, provided that  $L$  is greater than five years. The strong separability guaranteed by CiSSA and the generalization of Gray’s theorem [46], given in [18], justify the use of CiSSA with a non-stationary time series.

In CiSSA, the estimation of the trend-cycle component includes all the oscillations with periodicity greater than 18 months. Given the relationship between frequencies,  $\omega_k = (k - 1)/L$ , and elementary components, we keep all frequencies that yield cycles of periodicity greater than  $1/\omega_k = 18$  months. Therefore, we estimate the trend-cycle component for  $L = 96$  as the sum of the first six elementary components by frequency ( $\omega_1 = 0, \omega_2 = 1/96, \omega_3 = 1/48, \omega_4 = 1/32, \omega_5 = 1/24$  and  $\omega_6 = 5/96$ , corresponding to infinite, 96, 48, 32, 24 and 19.2 months, respectively) and, in a similar way, for  $L = 192$ , as the sum of the first 11 ones. The estimation of the AMB trend-cycle component is made in an automatic way, correcting for additive and transitory outliers.

Before we compare the accuracy of CiSSA and the AMB method, we need to check that both of them meet two conditions. First, the final point estimation of the cycle at time  $t$  is unbiased,  $E(\hat{c}_{t|t+K}) = c_t$ . And second, the preliminary point estimations of the cycle



converge to that unbiased final point estimation. Given  $P$  observations of  $r_{t|t+j}$  in each simulation, we define the distance

$$DFE_j = \left( \frac{1}{P} \sum_{t=2L+1}^{2L+P} r_{t|t+j}^2 \right)^{\frac{1}{2}}, j = 0, 1, \dots, K - 1$$

Then, it must hold that  $E(DFE_j) \rightarrow 0$  when  $j \rightarrow K$ . We observe that if the first condition holds, then the distance  $DFE_j$  is the root mean square error of  $\hat{c}_{t|t+j}$ .

Table 1 shows the percentiles of the distribution of the mean error in the final estimation of the cycle for the linear and non-linear models obtained by CiSSA, with window lengths  $L = 96$  and  $L = 192$ , and AMB methods. The central value of the distribution of the mean error is zero for both procedures, CiSSA and AMB, both in the linear and non-linear models for any window length. As a consequence, the final estimations are unbiased, both with CiSSA and AMB methods, and results are robust to the selection of  $L$ . Nevertheless, the AMB approach exhibits higher dispersion than CiSSA in the final cycle estimations. Both the interquartile range and the range between percentiles 95 and 5 are greater for the AMB method than for CiSSA, between 34 and 61% wider in the first case and between 46 and 65% in the second one.

**Table 1.** Percentiles of the mean error distribution of the final cycle estimation, in the simulations of the linear and non-linear models, estimated with CiSSA and AMB methods for  $L = 96$  and  $L = 192$ .

			Percentiles				
			5	25	50	75	95
Linear	$L = 96$	CiSSA	-0.00049	-0.00022	0.00000	0.00021	0.00052
		AMB	-0.00076	-0.00028	0.00002	0.00032	0.00088
	$L = 192$	CiSSA	-0.00182	-0.00086	-0.00007	0.00079	0.00185
		AMB	-0.00270	-0.00111	-0.00003	0.00110	0.00298
Non-linear	$L = 96$	CiSSA	-0.00052	-0.00019	0.00000	0.00020	0.00050
		AMB	-0.00085	-0.00033	-0.00001	0.00030	0.00083
	$L = 192$	CiSSA	-0.00197	-0.00079	-0.00001	0.00082	0.00197
		AMB	-0.00283	-0.00106	-0.00001	0.00116	0.00293

Figures 3 and 4 show the medians of the distribution of the distances  $DFE_j$  for the linear and non-linear simulations, obtained by CiSSA with window lengths  $L = 96$  and  $L = 192$  and by AMB methods. First, we can observe that, in all the situations, the medians converge to zero, both with CiSSA and AMB procedures. Therefore, both methods verify the second condition. However, we must highlight that the  $DFE_j$  medians for CiSSA are smaller than those for AMB methodology in all the preliminary estimations and that they converge to zero faster with CiSSA than with AMB method. The fact that, in terms of the median, the distance  $DFE_j$  is around 60% smaller in the CiSSA than in the AMB procedure for the initial estimation is very relevant for the real-time forecasts of the economic cycle.

Through simulations, we can obtain the distribution of the ratio given in Equation (2) to compare the magnitude of the revisions in the economic cycle between CiSSA and AMB procedures. Therefore, we can compute the probability

$$P_j = \Pr(RMR_j < 1), j = 0, 1, \dots, K - 1$$

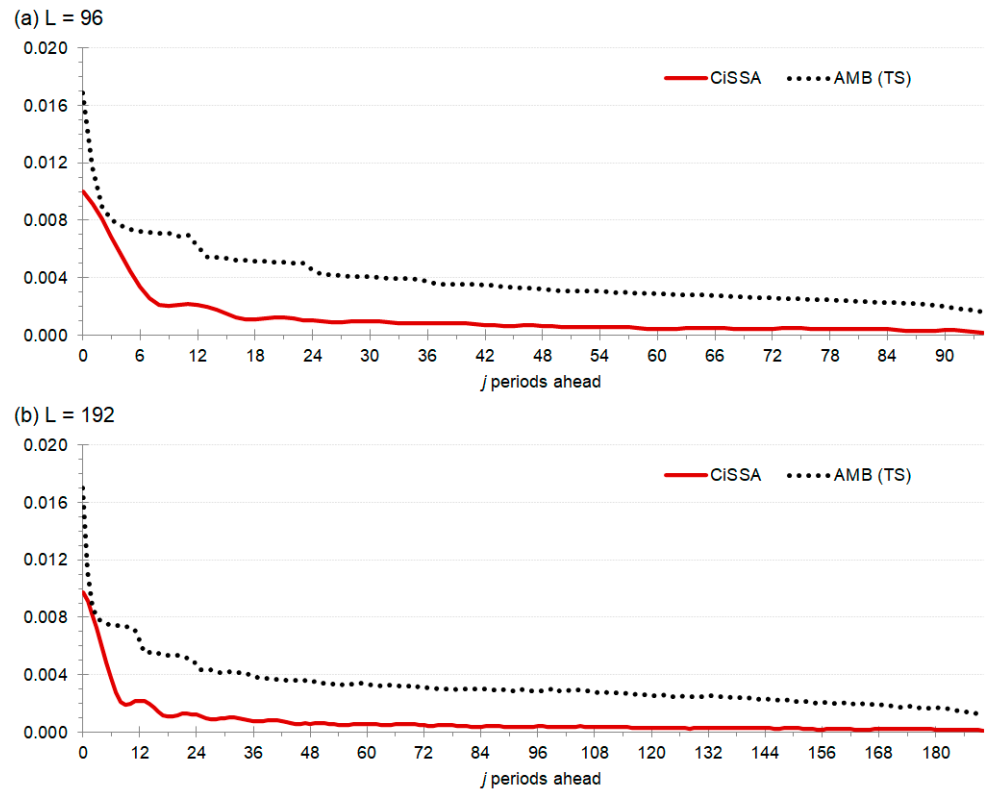


Figure 3. Median of the distance  $DFE_j$  in the linear model simulations estimated with CiSSA and AMB (implemented with TS) methods for the window lengths  $L = 96$  (a) and  $L = 192$  (b).

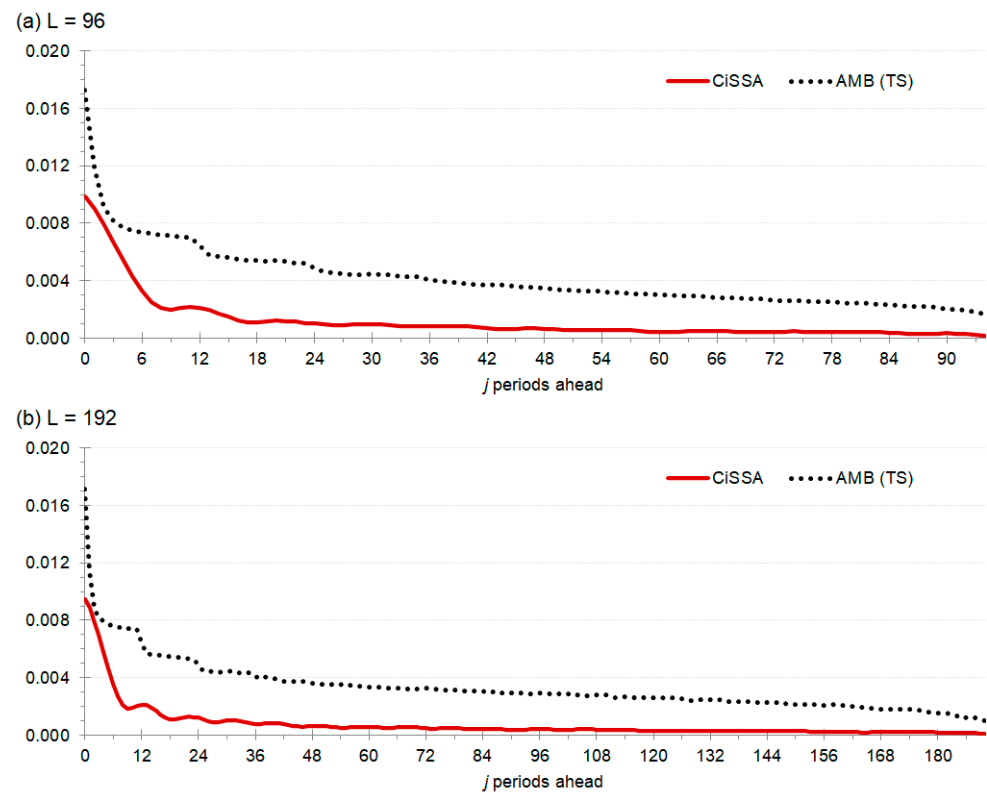
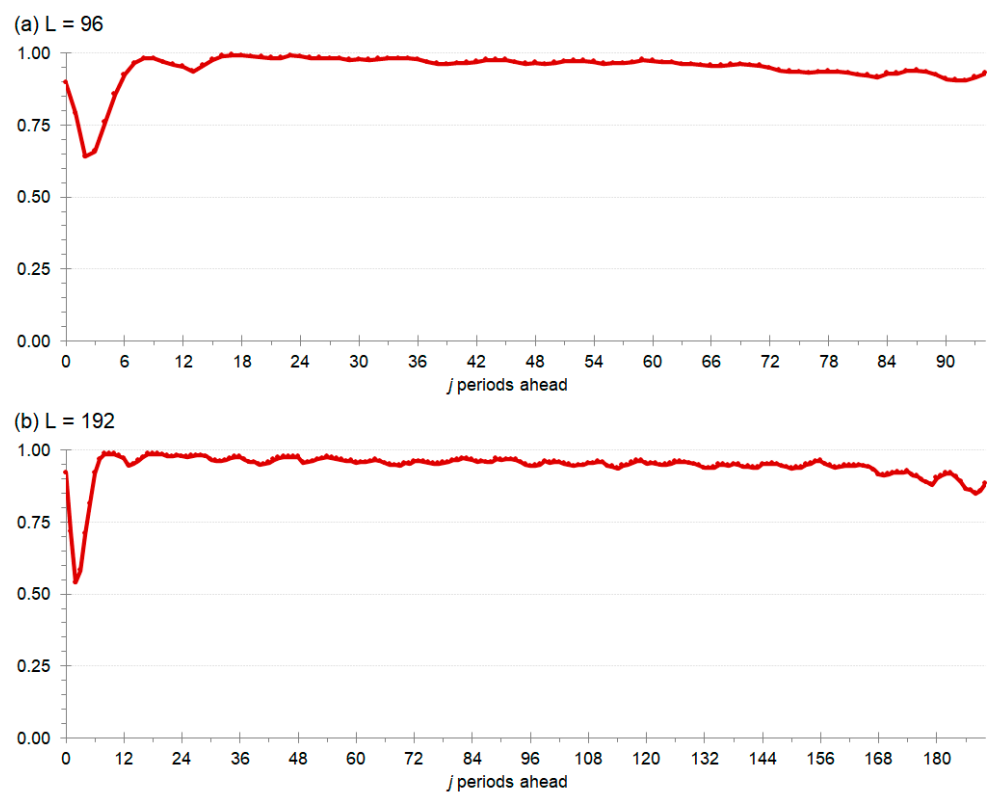


Figure 4. Median of the distance  $DFE_j$  in the non-linear model simulations estimated with CiSSA and AMB (implemented with TS) methods for the window lengths  $L = 96$  (a) and  $L = 192$  (b).

For a given  $j$ , if  $P_j > 0.5$ , we can say that CiSSA has greater probability to suffer fewer revisions than the AMB method in the preliminary estimation  $j$  periods after the initial estimation. If  $P_j > 0.5 \forall j \geq 0$ , then the CiSSA methodology provides a more stable estimation path, with fewer revisions than AMB methodology.

Figures 5 and 6 show the probabilities that the ratio  $RMR_j$  is less than one, for the linear and non-linear model simulation, in the cycle revisions obtained by CiSSA and AMB with window lengths  $L = 96$  and  $L = 192$ . All the graphs show that the probability is greater than 0.5 in every situation and for any horizon. It can be highlighted that the probability for the initial revision is equal or greater than 0.90 in all cases. Therefore, CiSSA generates cycle estimations that are accurate and suffer fewer revisions than those of the AMB procedure.

Notice that the relevance of the higher accuracy in the preliminary estimations results in a reduction of the uncertainty when forecasting in real time the economic cycle.



**Figure 5.** Probability that the ratio  $RMR_j$  is less than one in the linear model simulations for the estimations obtained with CiSSA and AMB (implemented with TS) methods with window lengths  $L = 96$  (a) and  $L = 192$  (b).

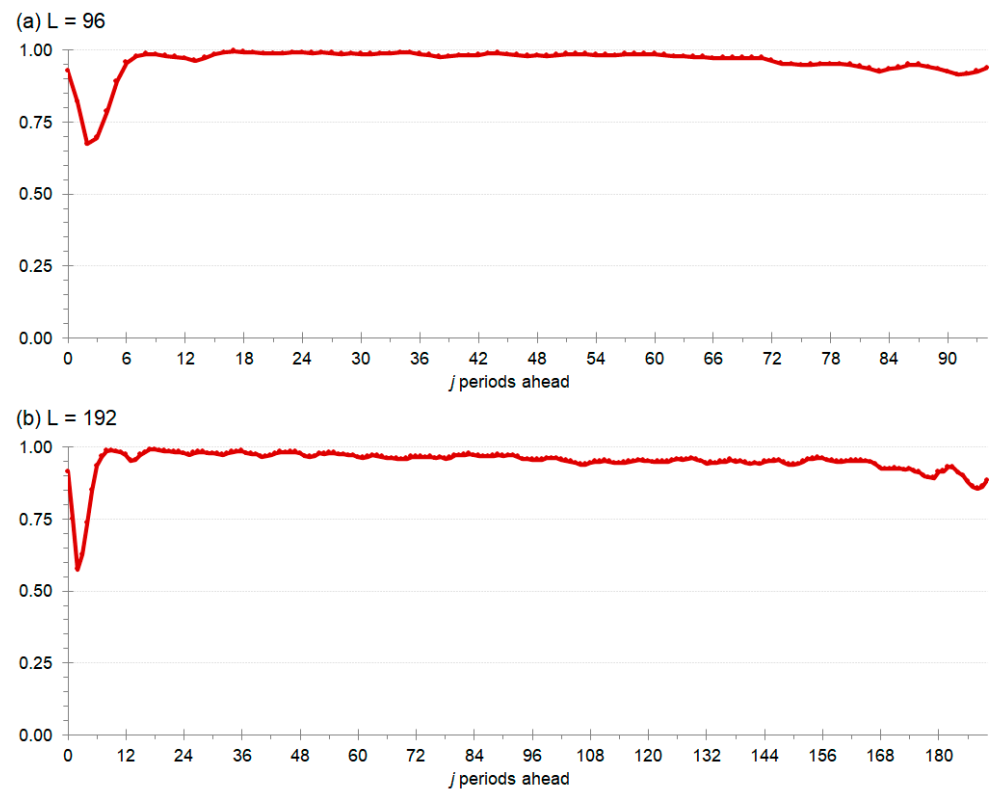


**Figure 6.** Probability that the ratio  $RMR_j$  is less than one in the non-linear model simulations for the estimations obtained with CiSSA and AMB (implemented with TS) methods with window lengths  $L = 96$  (a) and  $L = 192$  (b).

### 3.3. Empirical Application

Having analyzed the path of revisions of the underlying components of a time series through a set of simulations, in this subsection we check this issue with real data and evaluate the magnitude of the revisions in the estimated cycle component with the CiSSA and AMB methods for the Industrial Production (IP) index in France, Germany, Italy, Spain, United Kingdom and United States. IP data are extracted from the International Monetary Fund database, and the time span covers January 1970 to December 2019; therefore,  $T = 600$ . For CiSSA, we choose  $L = 96$  and  $P = T - 3L + 1 = 313$ . For Tramo-Seats estimation of the trend-cycle, we consider the automatic modelling with outlier correction. We take  $K = L - 1 = 95$ .

Figure 7 shows the evolution of  $RMR_j$  for different values of  $j$  for the six countries analyzed. As it can be seen, the ratio for  $j = 0$  in all countries is smaller than one, indicating that the real-time first estimation shows fewer revisions with CiSSA than with the AMB method. CiSSA shows less revision, except in Italy for three values of  $j$ . In fact, the average ratio is between 0.21 and 0.38. This means that the average magnitude of the revision is 70% smaller with CiSSA than the with the AMB method.

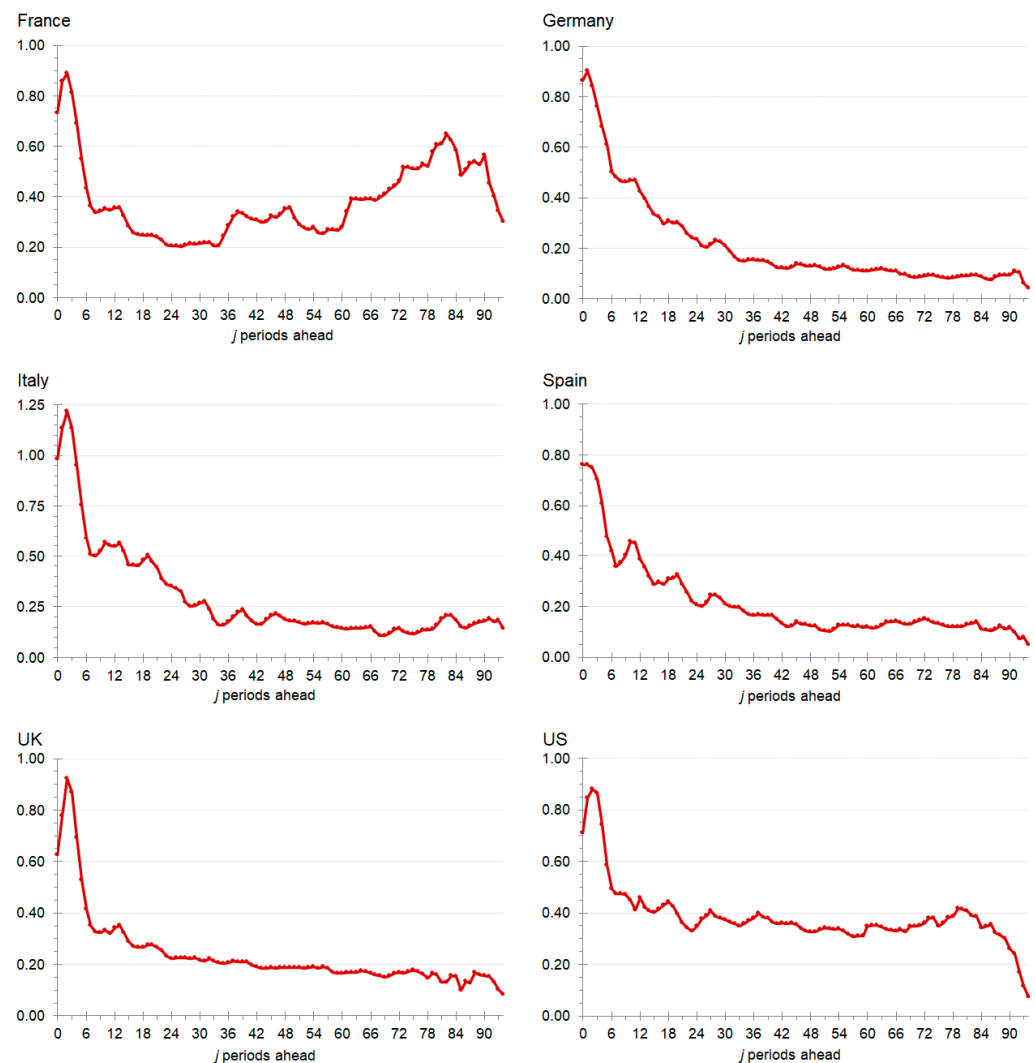


**Figure 7.** Ratio  $RMR_j$ ,  $j = 0, 1, \dots, K$  measuring the standard deviation of the revisions after  $j$  periods for IP with CiSSA ( $L = 96$ ).

To gain further insight in the evaluation of the revisions, Figure 8 shows the evolution of the cycle estimations for January 2008, a moment just before the crisis, along time for the different IP countries. The revision period is very tricky as it comprises two crises: the Great Recession starting in 2008 and the subsequent sovereign debt crisis in Europe in 2012–2015. These two unstable periods have very different effects on the revisions, depending on the method, as we see in the different countries. In general, the AMB approach seems more unstable, since revisions fluctuate more (see, for instance, the AMB graph for Italy, with spikes all over the revision path). In France, the effect of the 2008 crisis is very strong in the initial revisions, although the final data are about the same for both procedures. In the case of Germany, the graph shows that the AMB procedure heavily revises downwards the estimation of the data point for January 2008 after the introduction of the European sovereign debt crisis, starting in 2012.

The main conclusion is that CiSSA is more robust, and stability in the estimation is reached after two years, while AMB approach needs four years. After this stabilization period, the AMB method still continues to show some erratic behavior, while CiSSA remains more stable.

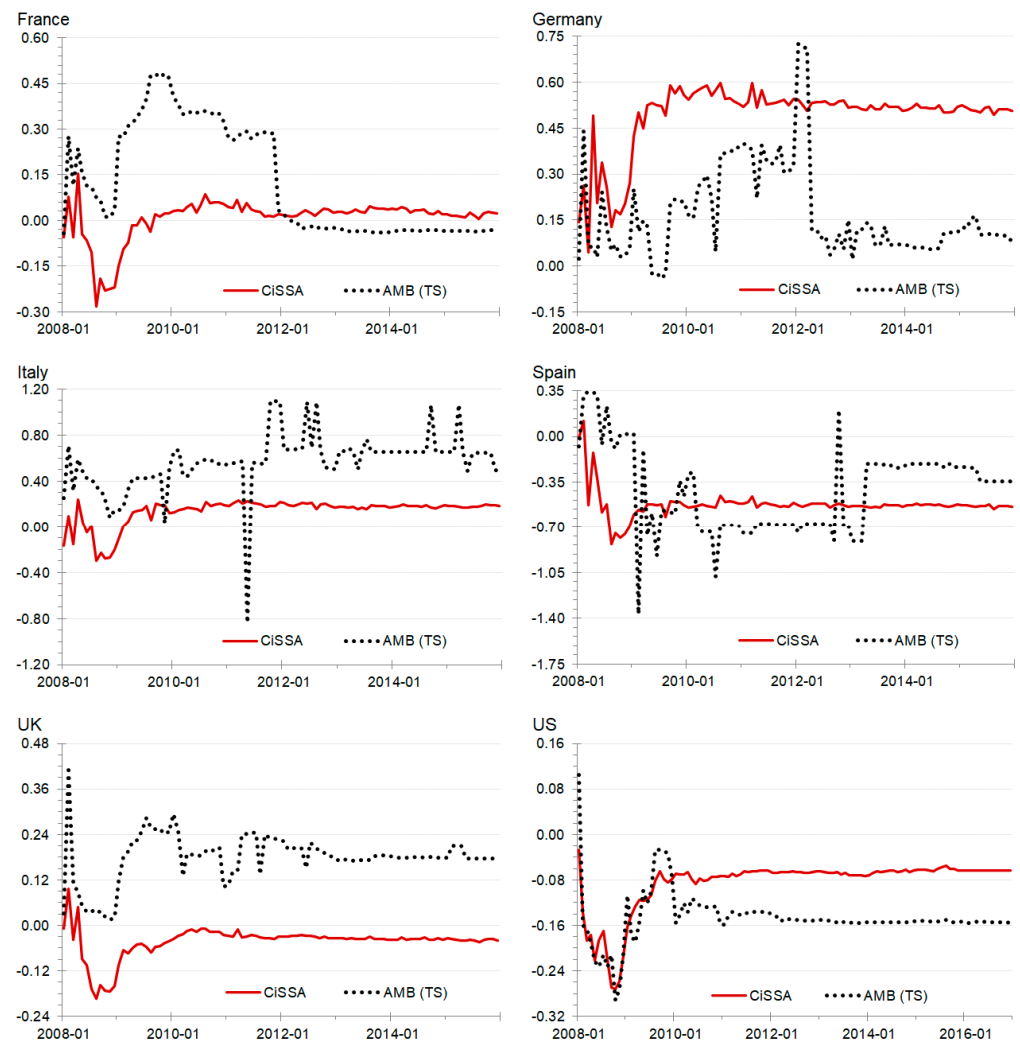


**Figure 8.** Revisions of the cycle estimation for January 2008 obtained by CiSSA ( $L = 96$ ) and AMB (implemented with TS) methods.

#### 4. Conclusions

From the point of view of policy makers, there are two characteristics that the extracted signals need to fulfill: timeliness and stability. Timeliness is required to give early policy responses, and stability is desirable to ensure the robustness of real-time decisions. Unfortunately, the earlier the estimation, the more likely that it will need revisions. Therefore, analysts and institutions need to reduce the uncertainty due to revisions when making decisions in real time. In this paper, we compare how two different signal extraction procedures behave with regard to revisions.

In order to address the previous concerns regarding signal extraction procedures for policy makers, we compare Circulant SSA, a non-parametric technique, with the widely used AMB parametric method, through a simulation study and an empirical analysis with real data.

From the simulation study, we conclude that the final estimates of the cycle at time  $t$  are unbiased in both procedures. Moreover, we also see that both procedures converge, although the speed of convergence of CiSSA to its final estimate is faster. Additionally, we find that CiSSA has a greater probability of smaller revisions than the AMB method. This would make CiSSA more appealing to policymakers, since more robust policy decisions could be made in shorter time. Moreover, the most important estimate for the analysis in real time, that is, the initial estimate, is closer to the final estimate with CiSSA than with the alternative parametric procedure. Therefore, the reaction of the analysts in real time would

be more similar to the one they would have had with the final estimate. Furthermore, the distribution of revisions with CiSSA shows less dispersion. As a consequence, the estimation path in the CiSSA framework is more stable than that of the AMB procedure. Therefore, CiSSA generates more reliable assessments of the business cycle in real time since they usually depend on the concurrent and first preliminary estimates. Consequently, decision-making with CiSSA is carried out with less uncertainty.

The assessment of the magnitude of the revisions was also analyzed with real data. Industrial Production is a monthly indicator, widely used to monitor the state of the economy, and is considered as one of the early warnings to detect turning points in the business cycle. The analysis in real time corroborates the overall result of the simulations. Moreover, it is useful to understand the nature of the revisions in a very special moment of time, January 2008, just before the Great Recession started. CiSSA provides a more robust assessment of the state of the economy in real time as its first estimation converges quicker to the last and with a more stable estimation path than the AMB alternative.

Finally, monitoring of the estimation path allows a continuous evaluation of economic policies and allows for determination of whether it is necessary to modify them in order to achieve medium- and long-term goals.

**Author Contributions:** Conceptualization, J.B., P.P. and E.S.; methodology, J.B., P.P. and E.S.; software, J.B.; validation, J.B., P.P. and E.S.; formal analysis, J.B.; investigation, J.B., P.P. and E.S.; resources, J.B., P.P. and E.S.; data curation, J.B.; writing—original draft preparation, J.B., P.P. and E.S.; writing—review and editing, J.B., P.P. and E.S.; visualization, J.B., P.P. and E.S.; supervision, J.B., P.P. and E.S.; project administration, E.S.; funding acquisition, J.B., P.P. and E.S. All authors have read and agreed to the published version of the manuscript.

**Funding:** This research was funded by the Spanish Ministerio de Ciencia e Innovación, grant numbers PID2019-107161GB-C32 and PID2019-108079GB-C22/AIE/10.13039/501100011033.

**Institutional Review Board Statement:** Not applicable.

**Informed Consent Statement:** Not applicable.

**Data Availability Statement:** Data were retrieved from the IMF web page <https://data.imf.org> (accessed on 23 March 2021).

**Conflicts of Interest:** The authors declare no conflict of interest. The funders had no role in the design of the study; in the collection, analyses, or interpretation of data; in the writing of the manuscript, or in the decision to publish the results.

## Abbreviations

AMB	ARIMA-model-based
ARIMA	AutoRegressive Integrated Moving Average
CiSSA	Circulant Singular Spectrum Analysis
GDP	Gross Domestic Product
MMSE	Minimum Mean Square Error
IP	Industrial Production
SSA	Singular Spectrum Analysis
TS	Programs TRAMO-SEATS
VAR	Vector AutoRegression

## Symbols

$\{x_t\}$ or $x_t$	Time series
$T$	Length of time series
$L$	Window length
$N$	Number of columns of the trajectory matrix
$\mathbf{x}_j = (x_j, \dots, x_{j+L-1})'$	Vector of length $L$ and origin at time $j$ obtained from $x_t$
$\mathbf{X} = (\mathbf{x}_1   \dots   \mathbf{x}_N)$	Trajectory matrix with columns $\mathbf{x}_j$

$s_m$	$m$ -th sample second moment
$\mathbf{S}_C$	Circulant matrix built with the sample second moments
$\lambda_k$	$k$ -th eigenvalue of the matrix $\mathbf{S}_C$
$\mathbf{u}_k$	$k$ -th eigenvector of the matrix $\mathbf{S}_C$ , $k$ -column of matrix $\mathbf{U}$
$\mathbf{U}$	The Fourier unit matrix
$\omega_k = \frac{k-1}{L}$	Frequency in cycles per unit time
$\mathbf{X}_k$	$k$ -th elementary matrix of rank 1
$B_k$	$k$ -th elementary pairs of frequencies
$\mathbf{X}_{B_k}$	Elementary matrix by frequency associated with the pair $B_k$
$I_j$	$j$ -th group de pairs $B_k$ linked to an unobserved component
$\mathbf{X}_{I_j}$	Matrix associated with the group $I_j$
$\tilde{x}_t^{(j)}$	Reconstructed/estimated series of an unobserved component
$c_t$	Business cycle at period $t$
$\hat{c}_{t t+j}$	Preliminary estimate of $c_t$ when data are available at time $t + j$
$r_{t t+j}$	Revision of the estimate of $c_t$ at time $t + j$
$K = L - 1$	Number of periods when there are no more revisions
$P = T - 3L + 1$	Number of preliminary estimates after $j$ periods
$\sigma(r_{t t+j})$	Standard deviation of the revisions after $j$ periods
$RMR_j$	Ratio of $\sigma(r_{t t+j})$ calculated by CiSSA and AMB methods
$E(\hat{c}_{t t+K})$	Mean of the final estimate of $c_t$
$DFE_j$	Root mean square error of $\hat{c}_{t t+j}$
$P_j = \Pr(RMR_j < 1)$	Probability that the $RMR_j$ ratio is less than one

## References

1. Croushore, D. Frontiers of Real-Time Data Analysis. *J. Econ. Lit.* **2011**, *49*, 72–100. [CrossRef]
2. Orphanides, A. Monetary policy rules based on real-time data. *Am. Econ. Rev.* **2001**, *91*, 964–985. [CrossRef]
3. Ashley, J.; Driver, R.; Hayes, S.; Jeffery, C. *Dealing with Data Uncertainty*. Bank of England Quarterly Bulletin; Spring: London, UK, 2005.
4. Damia, V.; Picón Aguilar, C. Quantitative Quality Indicators for Statistics—An Application to Euro Area Balance of Payment Statistics. In *Occasional Paper Series*; Paper No. 54; European Central Bank: Frankfurt am Main, Germany, 2006; Available online: <https://www.ecb.europa.eu/pub/pdf/scpops/ecbocp54.pdf> (accessed on 21 May 2021).
5. Fixler, D.J.; Nalewaik, J. *News, Noise, and Estimates of the “True” Unobserved State of the Economy*; Divisions of Research & Statistics and Monetary Affairs Federal Reserve Board: Washington, DC, USA, 2007. Available online: <https://www.federalreserve.gov/econres/feds/news-noise-and-estimates-of-the-quottruequot-unobserved-state-of-the-economy.htm> (accessed on 21 May 2021).
6. Diebold, F.X.; Rudebusch, G.D. Forecasting output with the composite leading index: A real-time analysis. *J. Am. Stat. Assoc.* **1991**, *86*, 603–610. [CrossRef]
7. Jacobs, J.P.; van Norden, S. Modeling data revisions: Measurement error and dynamics of “true” values. *J. Econ.* **2011**, *161*, 101–109. [CrossRef]
8. Dagum, E.B.; Bianconcini, S. *Seasonal Adjustment Methods and Real Time Trend-Cycle Estimation*; Springer International Publishing: Berlin, Germany, 2016.
9. Patterson, K.; Hassani, H.; Heravi, S.; Zhigljavsky, A. Multivariate singular spectrum analysis for forecasting revisions to real-time data. *J. Appl. Stat.* **2011**, *38*, 2183–2211. [CrossRef]
10. De Carvalho, M.; Rodrigues, P.C.; Rua, A. Tracking the US business cycle with a singular spectrum analysis. *Econ. Lett.* **2012**, *114*, 32–35. [CrossRef]
11. Conrad, W.; Corrado, C. Application of the Kalman filter to revisions in monthly retail sales estimates. *J. Econ. Dyn. Control.* **1979**, *1*, 177–198. [CrossRef]
12. Harvey, A.C.; McKenzie, C.R.; Blake, D.P.C.; Desai, M.J. Irregular data revisions. *Appl. Time Ser. Anal. Econ. Data* **1983**, 329–347.
13. Patterson, K.D.; Heravi, S.M. Data revisions and the expenditure components of GDP. *Econ. J.* **1991**, *101*, 887–901. [CrossRef]
14. Patterson, K.D. A state space approach to forecasting the final vintage of revised data with an application to the index of industrial production. *J. Forecast.* **1995**, *14*, 337–350. [CrossRef]
15. Orphanides, A.; van Norden, S. The unreliability of output-gap estimates in real time. *Rev. Econ. Stat.* **2002**, *84*, 569–583. [CrossRef]
16. Wildi, M. *Real-Time Signal Extraction*; Lecture Notes in Economics and Mathematical Systems, #547; Springer: Berlin, Germany, 2007.
17. Eurostat. Handbook on Seasonal Adjustment. 2018. Available online: <https://ec.europa.eu/eurostat/documents/3859598/8939616/KS-GQ-18-001-EN-N.pdf> (accessed on 21 May 2021).
18. Bógalo, J.; Poncela, P.; Senra, E. Circulant Singular Spectrum Analysis: A new automated procedure for signal extraction. *Signal Process.* **2021**, *179*, 107824. [CrossRef]



19. Dynan, K.E.; Elmendorf, D.W. Do provisional estimates of output miss turning points? *Board Gov. Fed. Reserv. Syst.* **2001**, working Paper.
20. Swanson, N.R.; Van Dijk, D. Are statistical reporting agencies getting it right? Data rationality and business cycle asymmetry. *J. Bus. Econ. Stat.* **2006**, *24*, 24–42. [[CrossRef](#)]
21. Golyandina, N.; Nekrutkin, V.; Zhigljavsky, A. *Analysis of Time Series Structure: SSA and Related Techniques*; Chapman & Hall/CRC: Boca Raton, FL, USA, 2001.
22. Harris, T.J.; Yuan, H. Filtering and frequency interpretations of singular spectrum analysis. *Phys. D Nonlinear Phenom.* **2010**, *239*, 1958–1967. [[CrossRef](#)]
23. Khan, M.A.R.; Poskitt, D.S. Forecasting stochastic processes using singular spectrum analysis: Aspects of the theory and application. *Int. J. Forecast.* **2017**, *33*, 199–213. [[CrossRef](#)]
24. Mahmoudvand, R.; Rodrigues, P.C. Missing value imputation in time series using Singular Spectrum Analysis. *Int. J. Energy Stat.* **2016**, *4*, 1650005. [[CrossRef](#)]
25. Broomhead, D.; King, G. Extracting qualitative dynamics from experimental data. *Phys. D Nonlinear Phenom.* **1986**, *20*, 217–236. [[CrossRef](#)]
26. Fraedrich, K. Estimating the dimension of weather and climate attractors. *J. Atmos. Sci.* **1986**, *43*, 419–432. [[CrossRef](#)]
27. Vautard, R.; Ghil, M. Singular spectrum analysis in nonlinear dynamics, with applications to paleoclimatic time series. *Phys. D Nonlinear Phenom.* **1989**, *35*, 395–424. [[CrossRef](#)]
28. Vautard, R.; Yiou, P.; Ghil, M. Singular-spectrum analysis: A toolkit for short, noisy chaotic signals. *Phys. D Nonlinear Phenom.* **1992**, *58*, 95–126. [[CrossRef](#)]
29. Safi, S.M.M.; Pooyan, M.; Nasrabadi, A.M. Improving the performance of the SSVEP-based BCI system using optimized singular spectrum analysis (OSSA). *Biomed. Signal Process. Control.* **2018**, *46*, 46–58. [[CrossRef](#)]
30. Yurova, A.; Bobylev, L.P.; Zhu, Y.; Davy, R.; Korzhikov, A.Y. Atmospheric heat advection in the Kara Sea region under main synoptic processes. *Int. J. Climatol.* **2019**, *39*, 361–374. [[CrossRef](#)]
31. Kumar, U.; Jain, V.K. Time series models (Grey-Markov, Grey Model with rolling mechanism and singular spectrum analysis) to forecast energy consumption in India. *Energy* **2010**, *35*, 1709–1716. [[CrossRef](#)]
32. Bozzo, E.; Carniel, R.; Fasino, D. Relationship between Singular Spectrum Analysis and Fourier analysis: Theory and application to the monitoring of volcanic activity. *Comput. Math. Appl.* **2010**, *60*, 812–820. [[CrossRef](#)]
33. Arteche, J.; García-Enríquez, J. Singular Spectrum Analysis for signal extraction in Stochastic Volatility models. *Econ. Stat.* **2017**, *1*, 85–98. [[CrossRef](#)]
34. Hassani, H.; Soofi, A.S.; Zhigljavsky, A. Predicting inflation dynamics with singular spectrum analysis. *J. R. Stat. Soc. Ser. A* **2013**, *176*, 743–760. [[CrossRef](#)]
35. Patterson, K.D.; Heravi, S.M. Revisions to official data on US GNP: A multivariate assessment of different vintages. *J. Off. Stat.* **2004**, *20*, 573–602.
36. Carvalho, M.D.; Rua, A. Real-time nowcasting the US output gap: Singular spectrum analysis at work. *Int. J. Forecast.* **2017**, *33*, 185–198. [[CrossRef](#)]
37. Kaiser, R.; Maravall, A. Estimation of the business cycle: A modified Hodrick-Prescott filter. *Span. Econ. Rev.* **1999**, *1*, 175–206. [[CrossRef](#)]
38. Canova, F. Detrending and business cycle facts. *J. Monet. Econ.* **1998**, *41*, 475–512. [[CrossRef](#)]
39. Hillmer, S.C.; Tiao, G.C. An ARIMA-model-based approach to seasonal adjustment. *J. Am. Stat. Assoc.* **1982**, *77*, 63–70. [[CrossRef](#)]
40. Kolmogorov, A. Interpolation und extrapolation von stationären zufälligen folgen. *Bull. Acad. Sci. USSR Ser. Math.* **1941**, *3*, 3–14.
41. Wiener, N. *Extrapolation, Interpolation, and Smoothing of Stationary Time Series with Engineering Applications*; MIT: Cambridge, MA, USA; Wiley: New York, NY, USA, 1949.
42. Cleveland, W.P.; Tiao, G.C. Decomposition of seasonal time series: A model for the census X-11 program. *J. Am. Stat. Assoc.* **1976**, *71*, 581–587. [[CrossRef](#)]
43. Young, P.C. *Recursive Estimation and Time Series Analysis: An Introduction*; Springer: Berlin, Germany, 1984.
44. Durbin, J.; Koopman, S.J. *Time Series Analysis by State Space Methods*, 2nd ed.; Oxford University Press: Oxford, UK, 2012.
45. Gómez, V.; Maravall, A. *Programs TRAMO and SEATS: Instructions for the User*; Working Paper 9628; Bank of Spain: Calle de Alcalá, Madrid, 1996; Available online: <https://www.bde.es/f/webbde/SES/Secciones/Publicaciones/PublicacionesSeriadadas/DocumentosTrabajo/98/Fic/dt9805e.pdf> (accessed on 21 May 2021).
46. Gray, R.M. On Unbounded Toeplitz Matrices and Nonstationary Time Series with an Application to Information Theory. *Inf. Control* **1974**, *24*, 181–196. [[CrossRef](#)]